Investigation of Mixing a Supersonic Stream with the Flow Downstream of a Wedge

NCC2-5190 Final Report

Joseph Sheeley
University of California, Berkeley
April 8, 1997

Table of Contents

Abstract

The flow characteristics in the base region of a two-dimensional supersonic compression ramp are investigated. A stream-wise oriented air jet, M=1.75, is injected through a thin horizontal slot into a supersonic air main flow, M=2.3, at the end of a two-dimensional compression ramp. The velocity profile and basic characteristics of the flow in the base region immediately following the ramp are determined. Visualization of the flowfield for qualitative observations is accomplished via Dark Central Ground Interferometry (DCGI). Two-dimensional velocity profiles are obtained using Laser Doppler Velocimetry (LDV). The study is the initial phase of a four-year investigation of base flow mixing. The current study is to provide more details of the flowfield.

Introduction

Traditional ramjet engines are the ideal choice of engines for flight at Mach numbers between three and 6.[1] Ramjet engines (figure 1) slow the supersonic free stream air to subsonic speeds through a series of oblique shocks and a final normal shock. These shocks are generated by the vehicle fore body and/or the diffuser. Fuel is then vaporized (if liquid) and burned in a subsonic burner before the main stream air and combustion products are accelerated to supersonic speeds through an exhaust nozzle. Function of the ramjet relies, in part, on the compression of the free stream air by the shock system to generate the high pressures needed for thrust. This shock system, however, can cause significant stagnation pressure losses, excessive temperatures and pressures in the combustion region and losses in available chemical energy due to molecular dissociation. These effects are particularly pronounced when the free stream Mach number exceeds about six.

These problems are bypassed in a scramjet engine (figure 2) by keeping the flow at supersonic speeds through the entire engine. New problems arise, however, with such a configuration. One such problem is that the air is only inside the combustion zone for a few milliseconds before being shot out the rear of the engine, and mixing the fuel and the air so that efficient, stable combustion can occur is difficult. It is estimated that mixing must occur within 1 millisecond inside a scramjet combustor of reasonable length.[15] The mixing problem has been the work of many investigators.

One mixing technique is the use of compression ramps or contoured wall injectors. Such injectors consist of a ramp that may have straight edges or be swept, the end of the ramp being narrower than the start. At the end of the ramp fuel is injected parallel to the freestream through the face whose normal is oriented in the streamwise direction. Such injectors may be used alone, or in a group, forming a series of ridges and troughs.[11] Oblique shocks are formed at the start of the ramps and in the troughs for a group of ramps, which interact with the interface between the freestream and injected flow, causing streamwise oriented vorticity. Vorticity may also be generated by the pressure gradient between the face of the ramp and the trough.[8,15]

The region immediately after the ramp is called the "base region," and is the region investigated in this report. Relatively little has been published on the flow in this region, although a considerable amount of work has been done on contoured wall injectors overall. Riggins *et al.*[8] noted some effects of this region on the flow, but did not discuss their cause. One such effect noted is the change in the orientation of vorticity shed by the ramps.

This report assumes the reader is familiar with compressible fluid dynamics, but has little experience with contoured wall injectors. A brief overview of the work of previous investigators is presented in the next section of this report. A more in-depth discussion follows, taken from the important results of previous studies, beginning with the basic combustion aspects with a very simple shear layer geometry, then going into the effect of more complex geometries on mixing for

flows without combustion, and concluding with a detailed discussion of the effects of ramp injectors on mixing without combustion. Finally, experimental results from tests on the base region are given, followed by conclusions drawn from these tests.

Previous Investigations

The basic aspects of mixing via diffusion and the chemical kinetics of combustion for a parallel, H_2-Air mixing layer were investigated numerically by Da Silva, Deshaies, and Champion.[2] The authors began with the steady boundary layer equations for a multi component, reactive flow. Included were conservation equations for total mass, streamwise momentum, energy, and species, along with perfect gas equations of state. Detailed chemical kinetics were modeled by equilibrium reaction equations involving nine species and thirty-eight elementary reactions. The resulting system of parabolic partial differential equations was solved numerically in (x^*, Ψ) space after a Von Mise's transformation (x, y) → (x^*, Ψ). The effects of viscosity and relative fluid temperatures on induction length were determined. Ju and Niioka[12] investigated the same configuration with a more extensive analytical investigation before employing numerical techniques on the problem with similar results.

Kwok *et al.*[3] investigated experimentally the mixing characteristics of helium/air and air/air injection/mainstream systems. The investigators injected air into air and helium into air through a slot, and compared the results. It was found that helium mixed more efficiently than air when injected at the same Mach number.

One of the first investigations of the effect of streamwise oriented vorticity on mixing -- the chief mixing mechanism of compression ramp injectors and indeed most supersonic mixers -- was done by Provinelli *et al.*[5] in 1969. Helium was injected into the streamwise oriented vortex generated by a highly swept delta wing. Provinelli and Hersch[6] performed a follow-up investigation, injecting helium at the confluence of two counter rotating vorticies generated by converging delta wings.

Many experimental and computational tests of compression ramps have been done in joint projects between the California Institute of Technology and NASA Langley Research Center. Among these is a study by Waitz, Marble, and Zukoski.[11] The authors investigated effects of boundary layer height between compression ramps, ramp/injector spacing, and injectant to freestream pressure and velocity ratios. Simulated and performed is the injection of helium at M=1.7 into a freestream at M=6 through an array of injector ramps placed side by side, forming ridges and troughs.

The first investigation of a swept ramp injector was done by Swithenbank *et al.*[7], with promising results. Riggins *et al.*[8] numerically investigated a swept ramp injector with M_∞=13.5 and a flush wall jet with M_∞=17. Kraus and Cuttler[9] investigated the effect of swirling the injectant by sending helium through vanes before injection at 30° to the freestream into a flow at M_∞=2.

A comprehensive numerical investigation of contoured wall injectors is presented by Riggins and Vitt.[10] Included are a description of the generation and evolution of vorticity from injector ramps and a method for the determination of the ideal combustor length to maximize thrust. Both swept and unswept ramps are modeled and compared. Among the most important revelations of this

work are the comparisons of mixing efficiency between laminar and turbulent freestream cases, and between turbulent flows with and without ramp generated vorticity.

An investigation of another promising method of vortex generation was done by Belovich *et al.*[4] The investigators used lobed injectors to generate vorticity. Results of this investigation are applicable to ramp injectors in that the effect of increasing axial vorticity on mixing is included. A theory concerning the interaction of streamwise vorticity and Kelvin-Helmholz instability induced structures is presented.

The important results from these investigations are presented in the next three sections. The results from Da Silva, Deshaies, and Champion[2] for the very basic geometry of a H_2/air reacting shear layer are presented first.

Combustion Aspects

Da Silva *et al.*[2] and Ju and Niioka[12] numerically investigate the mixing and subsequent combustion of an air-H_2 mixing layer (Figure 3). Da Silva *et al.*[2] relies upon mostly numerical techniques, while Ju and Niioka[12] provides a more in depth analytical analysis before numerical techniques are employed to solve the resulting equations. While the two papers gave similar results, Da Silva's presentation contains greater insight into the physical processes involved, and much of this section, therefore, is based upon Da Silva *et al.*

The analysis begins with the conservation equations for the multi-component, steady, compressible flow of a perfect gas:

$$\textit{Mass:}\quad (\rho u)_x + (\rho v)_y = 0 \qquad (1)$$

$$\textit{Momentum:}\quad \rho u u_x + \rho v u_y = -p_x + (\mu u_y)_y \qquad (2)$$

$$\textit{Energy:}\quad \rho u c_p T_x + \rho v c_p T_y = u p_x + \sum_{\alpha=1}^{K} \rho Y_\alpha V_\alpha C_{p_\alpha} T_y + \mu u_y^2 - \sum_{\alpha=1}^{K} h_\alpha \omega_\alpha + (\lambda T_y)_y \qquad (3)$$

and

$$\textit{Species:}\quad \rho u (Y_\alpha)_x + \rho v (Y_\alpha)_y = -(\rho Y_\alpha V_\alpha)_y + \omega_\alpha;\ \alpha = 1,2,\ldots,K \qquad (4).$$

The boundary conditions are:

$$x=0 \rightarrow \left\{ \begin{array}{l} y>0:\ \ Y_{H_2}=0,\ Y_{air}=1,\ u=U_{air},\ T=T_{air} \\ y<0:\ \ Y_{H_2}=1,\ Y_{air}=0,\ u=U_{H_2},\ T=T_{H_2} \end{array} \right\} \qquad (5)$$

and

$$\forall x \rightarrow \left\{ \begin{array}{l} y\rightarrow +\infty:\ \ Y_{H_2}=0,\ Y_{air}=1,\ u=U_{air},\ T=T_{air} \\ y\rightarrow -\infty:\ \ Y_{H_2}=1,\ Y_{air}=0,\ u=U_{H_2},\ T=T_{H_2} \end{array} \right\} \qquad (6).$$

Since the equations are two dimensional, the mass conservation can be satisfied identically by introducing a stream function, Ψ:

$$\frac{\partial \Psi}{\partial y} = u, \qquad -\frac{\partial \Psi}{\partial x} = v. \quad (7a,b)$$

Ψ=0 is then chosen to correspond with y=0. These, equations, along with equilibrium reaction equations for 38 elementary reactions involving 9 species, are solved numerically by Da Silva *et al.*[2]

A schematic of a typical air/hydrogen mixing layer is presented as figure 4. The stoichiometric line is displaced upwards since 2.36 air moles are required for each H_2 mole.[2] For this reason, combustion develops first on the air side of the layer, somewhere downstream of the initial air/H2 contact point, in the vicinity of the stoichiometric line.

An interesting phenomenon was noted by both Da Silva *et al.*[2] and Ju and Niioka.[12] As the velocity ratio, V_{air}/V_{H2}, was increased from an initial low value, the induction length increased and the flame front moved downstream as would be expected. When the velocity ratio was increased above a certain value, however, the flame front began to move up stream and the induction length *decreased.* Da Silva *et al.*[2] hypothesized that while convection increases induction length as velocity ratio increases, viscous heating causes the temperatures of the two streams to rise, causing a decrease in induction length. While convection is initially the dominant factor in determining induction length, viscous heating eventually overwhelms convection as the dominant factor at high velocity ratios and induction length decreases.[2] It was also noted that increasing the temperatures of one or both gasses before combustion decreased induction length.[2,12]

The combustion described in this section is for the very simple case of an H_2/air shear layer. The effects on the velocity profile and species concentration of the flow by various geometrical considerations is not considered. The next section describes the effect of various geometries on mixing between the fuel and the freestream for flows without the added complication of combustion.

Aspects of Mixing Enhancement

There are many factors that contribute to the mixing between an injected stream and a supersonic freestream. Among contributing factors are the presence of vorticity in the flow, the fuel-air velocity ratio, the ratio of jet entrance pressure to the main stream pressure, the fuel equivalence ratio, and the baroclinic effect of shock waves passing through jet plumes and interacting with boundary layers.[10] Other factors which can contribute to mixing include the diffusion rates of the mainstream and injected gasses,[2] the relative temperature of the main and injected streams,[2] interfacial area,[4] injectant swirl,[9] and angle of injection.[8,9] There are many secondary effects, such as the interaction between vortices generated by injector ramps and Kelvin-Helmholtz structures.[4]

One difficulty which arises in the study of supersonic mixing is the development of a means to judge the effectiveness of a configuration. One quantity often measured is jet penetration depth.[8,9,11] Such a quantity is easily observed and measured, since the injected flow can be marked with particles whose position can be determined by some optical means. If the particles are a visible smoke or mist, for example, a photograph of the flow can be taken and the jet penetration depth measured directly, perhaps via a software package.

The drawback of using penetration depth as the sole measure of mixer effectiveness, however, is that the quantity is highly dependant upon the initial cross-stream momentum of the injectant gas. Factors such as injectant entrance velocity, pressure, and angle can strongly influence jet penetration depth,[9] possibly skewing results. Other factors such as average injectant plume cross-sectional area (resulting in greater interfacial area and thus more mixing) and the decay of the maximum injectant concentration[9] (measured with rakes of probes).

Various other gages can be used with numerical investigations . Waitz, Marble, and Zukoski[11] calculate the variation in length of contours of constant max fraction vs. downstream distance, and the fraction of total mass flux of injectant gas at a given concentration as a function of downstream distance,

$$\frac{(\frac{\partial m}{\partial t})|_{Ci}}{(\frac{\partial m}{\partial t})|_{Ci-total}} \quad vs. \quad x \qquad (8)$$

where Ci is a given concentration of injectant gas.

Riggins and Vitt[19] define a factor, "vortex stirring length," defined as:

$$L_{vs} = \int \frac{|q_{cross}|}{U_{avg}} dx \qquad (9)$$

where q_{cross} is the average velocity in the cross-stream direction and U_{avg} is the average velocity of the flow (main and injected) in the freestream direction. The integration is performed from the injection point to the end of the combustor. L_{vs} is a measure of the average distance a particle travels in the cross-flow direction from the base of the injector to the combustor exit. A linear relation exists between the vortex stirring length and the amount of mixing.[10]

Variation in injection angle relative to the freestream has been studied, with configurations ranging from parallel injection to injection at 90° to the freestream. Strategies which inject fluid at 90° to the freestream, or transverse injectors, rely upon direct injectant interaction with the freestream to cause convective mixing.[11] Transverse injectors cause effective mixing, but do not add momentum to the flow, and can cause large stagnation pressure losses.[9]

Injection parallel to the freestream adds momentum to the freestream, thereby adding to thrust.[8,9] This contribution to thrust can be significant, even when compared to the thrust gained by chemical reactions.[8] For any practical hypersonic combustor, a significant component of momentum must be in the freestream direction to augment thrust.[11]

Two popular methods for producing counter rotating vortices are injector ramps and flush wall injectors.[10] Both methods rely upon strong pressure gradients in the flow produced by shock waves generated by the presence of the injector. Ramp injectors induce a high pressure region on the face of the ramp, behind a strong ramp bow shock. Flush wall jets generate a high pressure region on top of the jet plume itself behind the injector bow shock.[10] It should be noted that pressure gradient induced vorticity is only generate by three-dimensional ramps and jets -- the compression ramps and flush wall jets must be finite in the crosswise direction since these vortices are shed off of the sides of the ramps/jets.

Pressure gradients are only one of the mechanisms which generate axial vorticity about injector ramps and flush wall injectors. Complex jet shear and momentum effects also contribute to stream-wise oriented vorticity generation in flush wall injector configurations.[10] The shocks generated around contoured wall injectors (ramp injectors) interact with the density gradients existing in the mixing layer causing a baroclinic torque.[11] Further discussion on vorticity generation by compression ramps may be found in the section of this report dedicated entirely to contoured wall injectors.

Fortunately, the counter rotating vortex pair generated by contoured wall injectors and flush wall

injectors rotates in a manner as to lift the injectant layer off of the wall and enhance mixing.[11] The vorticity generated by all sources combines into a strong pair of vortices soon after the injection point. Mixing is greatly enhanced downstream where the vortices break down, causing a region of increased turbulence.[4] For this reason, mixing near the base region of the injector is dominated by the amount of interfacial area, while mixing downstream is dominated by the amount of vorticity in the flow.[4]

Waitz *et al.*[11] found that axial vorticity was more efficient at convecting an injectant of low relative momentum than higher relative momentum into the freestream. Therefore jet pressure ratios equal or less than unity were deemed best for loss effective mixing and good jet penetration in parallel injection. Belovich *et al.*[11] found, however, that the mixing enhancement due to vorticity as compared with that caused by interfacial area increases as the jet to freestream velocity ratio increases.

Swirling the injectant prior to injection is also found to have favorable effects on mixing. Kraus and Cutler[9] found that swirl increases mixing in parallel of near parallel injection. Performing experiments with helium and air, it was found that swirl significantly increased the cross-sectional area of the injectant plume, thus increasing mixing. It was found, however, that while swirl slightly increased penetration height for helium, penetration height for air injection was actually decreased when the injectant flow was swirled.

Finally, the effect of the thickness of the supersonic boundary layer on the wall is investigated by Waitz *et al.*[11] The authors found the boundary layer affected mixing by:

1) Modifying the effective wall geometry
2) Adding shear to the mixing region
3) Influencing axial vorticity production by turning the axial vorticity in the boundary layer
4) Adding unsteadiness to the mixing layer.

It was found that the effect of the boundary layer varied with injector spacing.[11] The boundary layer hindered mixing with closely spaced injectors (trough width equal to ramp width) by weakening secondary flow caused by ramps and hindering shock formation at the exit plane in the troughs. The boundary layer actually enhanced the secondary flow and didn't interfere with shock generation for a widely spaced (trough width equal to three ramp widths) injector geometry. The boundary layer interacted positively with the ramps, causing regions of high momentum fluid at the corners of the troughs, leading to strong baroclinic vorticity generation.

Having concluded a discussion of combustion for a simple geometry, and the effect of more complicated geometries on mixing for a non-reacting flow, the discussion now turns to the effect of the very specific geometry of injector ramps on a non-reacting flow.

Ramp Injectors

One effective means of vorticity generation is through the use of compression ramps (figure 5), also called "contoured fuel injectors." Contoured wall injectors generate axial vorticity through a variety of mechanisms. These mechanisms include: 1) baroclinic torque caused by shock impingement on the fuel/air interface,[11] 2) "spillage" between the shock pressurized ramp face and the lower pressure troughs beside injectors,[10] 3) Variation in cross-flow shear between the injected stream and the freesream in the exit plane due to secondary, ramp induced flow,[11] and 4) the turning and stretching of vortex lines associated with the incoming freestream wall boundary layer.[11] Cross-flow shear and baroclinic torque are particularly effective at enhancing mixing vorticity is generated directly at the interface.[11]

Physical insight into some of these mechanisms can be gained through the examination of the vorticity equation, derived by taking the curl of the momentum equation (see, for example, Batchelor, 1967[13]):

$$\frac{D\omega}{Dt} = \omega \cdot \nabla \boldsymbol{u} - \omega(\nabla \cdot \boldsymbol{u}) + \frac{\nabla\rho \times (\nabla P)}{\rho^2} + \frac{\rho \nabla \times (\nabla \cdot \tau) - (\nabla\rho \times \nabla \cdot \tau)}{\rho^2} \qquad (10).$$

The first term on the right side of equation (10), $\omega \cdot \nabla \mathbf{u}$, is the rate of change of the vorticity of a fluid element due to the turning and stretching/contraction of vortex lines.[18] The third term is the generation of vorticity due to baroclinic torque. This occurs wherever ∇P and $\nabla \rho$ are not parallel, such as where an oblique shock crosses the fuel/air interface.[11]

The final term in equation (10) is the generation of vorticity on the walls of the compression ramp and tunnel. This becomes apparent when the y-momentum equation is applied at the sides of the ramp ($\mathbf{u}=0$) with the viscous forces, represented by τ in (10), written out:

$$\frac{\partial p}{\partial y} = (\mu v_z)_z \qquad (11)$$

where v is the velocity component in the y direction and x, y, and z are oriented as shown in figure 6.

A secondary flow in the y direction between the ramp face and trough is generated by the pressurization of the ramp face, and a thin layer of stream-wise oriented vorticity is generated along the sides, which is shed from the ramp and convected downstream. Vorticity is also generated on the top and side faces of the ramp by the pressure gradient in the x direction which

exists throughout the flow, but this vorticity is oriented in the cross-stream direction. The orientation of vorticity may be changed after the ramps by base region effects and ramp induced flows,[10,11] leading to both increases and decreases in stream-wise oriented vorticity at different distances from the end of the ramps.

Provinelli *et al.*[5] found that mixing increased with increasing axial vortex strength. Riggins and Vitt[10] discovered that the removal of ramp generated vorticity numerically resulted in a 40% decrease in mixing efficiency (as measured by vortex stirring length, L_{vs}) by the middle of the combustor. Vortices shed from the sides of the ramps increase in strength as the ramp face/trough pressure ratio increases.[10] Swithenbank *et al.*[7] showed that 30% higher ramp face/trough pressure ratios could be produced by sweeping ramps (figure 7), but Waitz *et al.*[11] found that losses were greater with swept ramps than unswept ramps .

A graph showing the circulation strength as a function of downstream direction for a typical contoured wall injector is presented as figure 8.[8] Circulation due to vortex shedding increases linearly over the length of the ramp, decreases sharply in the base region where injection and base effects turn vorticity from the stream-wise direction, and then increases again as vorticity is turned in the stream-wise direction again.[10] The fuel/air interface is stretched by axially directed vorticity as the vortex pair lifts the fuel from the wall, and thus mixing is enhanced.[10] Viscous effects at the walls may reduce stream-wise circulation by as much as one third, but vorticity strength at the center of the combustor, where mixing occurs, remains fairly constant, owing to the relatively low viscosity of air and combustion gasses.

Although effects on the surface of the ramp and after the base region have been studied extensively, as evidenced by the material of the last three sections, little is known about the base region itself. The details of an investigation performed by this author into the flow in the base region of a two-dimensional compression ramp using various optical techniques, and results and conclusions gained through this investigation make up the rest of this report.

Experimental Apparatus

Wind Tunnel:

All tests were done in the Ames 15x15 cm continuous supersonic wind tunnel located at the University of California at Berkeley. The tunnel is closed cycled, and able to produce continuous, supersonic flow for several hours at Mach numbers ranging from 1.5 to 2.8. Changes in Mach number are accomplished by switching interchangeable, one-sided nozzle blocks[18].

Both stagnation pressure and temperature may be adjusted. The stagnation pressures possible range from about 2 to 22 psia ($1.3*10^4$ to $1.5*10^5$ N/m^2). Stagnation temperatures are possible from 60 to 80 degrees Fahrenheit (16 to 27 degrees Celsius). Large tanks of dried air supply additional mass when necessary to increase stagnation pressure. Adjustments to stagnation temperature, allowing the tunnel to be run at high Mach numbers, are possible by changing the amount of cooling water flowing through cooling pipes in the settling chamber[18].

At maximum stagnation temperature, pressure, and Mach 2.8, the mass flow rate through the test section is about 2 kg/s. All LDV experiments for this study were performed at a stagnation temperature of 21 °C and a stagnation pressure of 5 psia (34.5 kPa). The Mach number of the freestream flow is fixed at 2.4. Under these conditions, the mass flow rate of the free stream through the test section is about .66 kg/s. The injected flow is about .38 kg/s. DCGI is also performed at a stagnation pressure of 10 psia, all other conditions fixed, with a free stream mass flow rate is 1.32 kg/s.

The freestream boundary layer on the bottom of the tunnel is removed by suction just before the test section, allowing for a thin boundary layer at the beginning of the test section. The tunnel is driven by a 700 HP electric motor. A vacuum pump allows for operation below atmospheric pressures.

Model:

The model is shown as figure 10. The model is constructed entirely of aluminum which allows for a sharp "knife edge" at the beginning of the ramp, in turn allowing the production of a sharp oblique shock which is consistent in the cross-tunnel direction. The model is constructed in three pieces: 1. the ramp and plenum, 2. the nozzle bottom, 3. the nozzle top. This allows easy adjustment of the injected flow by simply changing the top or bottom of the nozzle, and thereby adjusting the throat and/or exit area, without refabrification of the entire model.

The plenum in the wedge is connected to a high pressure source (actually, the low pressure in the

test section, <2 psia, allows the room to be used as the high pressure source). Air fills the plenum, is drawn through a converging/diverging nozzle, and is injected at M=1.75 parallel to the mainstream flow. Although water vapor is present in the air which is injected, no ice has been observed to form. Perhaps the fraction of water vapor to freestream and injected air is too small to cause any noticeable effects.

Instrumentation:

Only optical instrumentation was used to take measurements, allowing unobtrusive measurements. Flow visualization is accomplished using Dark Central Ground Interferometry (DCGI). Velocity measurements were made using Laser Doppler Velocimetry (LDV).

A diagram of the DCGI system is shown as figure 9. DCGI, unlike other forms of interferometry, allows for real-time observation of the flowfield. The secret to the technique is to place a filter, such at a piece of a glass holographic plate, at the focus point of the laser after the beam has been passed through the test section. Initially all light passes through the filter, and a shadowgraph is formed. The intensity of the laser is then increased for several seconds until a dark spot is burned into the plate by the laser. This spot then blocks some of the light passing though the plate, causing and interferomic effect. More details on this technique may be found in Loomis and Holt[14] and Loomis, Holt, Chapman, and Coon[15] .

A diagram of the LDV is presented as figure 11. The system used was designed and developed by Aerometrics Corporation. Back-scatter was initially attempted, but it was found that the light reflected backwards was too faint, and the signals gathered by the photo detector were obscured in noise. A forward-scatter setup, as depicted in figure 11, was therefore decided upon, and worked fairly well except very close to the wall where reflections were a problem, and areas where sufficient seeding could not be obtained.

The main flow was seeded with water vapor from a humidifier through a valve after the cooling section. The injected flow was seeded with water vapor by injecting vapor produced by a commercial seeder into the pipe leading to the plenum. Sampling rates of 160 MHZ were used when the flow was around 400 m/s, and 80 MHZ when the flow velocity was below 200 m/s. Only the component of velocity parallel to the freestream was taken.

Results

Laser shadowgraph and DCGI pictures are presented as figures 12 and 13, and schematics of the flow are given a figures 14 and 15. In figures 12 and 14, the injection is turned off. A strong oblique shock is formed at the beginning of the ramp. The oblique shock begins to spread out and weaken about halfway to the top of the tunnel. The oblique shock reflects off the ceiling of the test section just before the end of the test section window (the right edge of the photograph).

A small expansion fan is visible near the end of the model where the model face turns parallel to the free stream flow. A much larger expansion fan lies at the end of the model, as the flow expands into the base region at the end of the model. A boundary layer appears along the model and in the base region as a dark shadow.

In figure 13, air is injected into the base region at the end of the ramp. The diamond shaped patterns to the right of the injection nozzle, consisting of alternating expansion fans and oblique shocks reveal that the injected flow is under expanded, as is expected, as it leaves the nozzle. A small, dark semicircle at the exit of the injector nozzle before the expansion/shock pattern also reveals a region of high pressure and high density.

The expansion fan at the end of the model is lifted upwards, and interacts with the smaller expansion fan. The boundary layer from the top of the model separates and is lifted upwards. This would suggest that the main stream/injected air interface would also be lifted upwards -- an encouraging sign. This would suggest a stretching of the fuel/air interface in a hydrogen injection system, which would promote mixing.

Seeding for the LDV measurements proved difficult. Initially, commercial smoke fluid was used, vaporized by a seeder and injected into the flow just past the cooling chamber through a long rod with several holes along its length, in an attempt to release the seed across the flow. This method failed to provide adequate seeding for the main flow.

Next, smoke was injected through a valve just past the cooling chamber. This method provided better results, but the windows of the tunnel would quickly coat with the condensed fluid, and the tunnel would need to be shut down so that the windows could be cleaned. Feather balls and powder were also tried, but these either would coat the windows too rapidly, or be too small to provide signals which could be separated from the noise.

Finally, water vapor from a humidifier was injected into the main flow through a valve, and this proved adequate. For the injected flow, some measurements were accomplished seeding the main flow with the humidifier and seeding the injected flow with water from the seeder, while other measurements deep in the injection region were accomplished simply by supplying water vapor from the humidifier into the injected air. Even with the large amounts of water vapor inserted into the flow with this technique, it was difficult to get velocity readings near the walls and at certain

parts of the flow with injection due to noise and reflection off the walls.

The velocity measurements in the streamwise direction are provided as figures 16 and 17. In figure 16, the jet is off, and a large recirculation region follows the model, in which regions of back flows with speeds of several tens of meters per second are present near the walls. This region is very turbulent, with particles of many velocities found in this region. The region above this recirculation zone, but still below the top of the model also was highly turbulent, with a wide range of velocities.

Velocity measurements for the flow in the freestream above the model were taken with the jet turned off. The freestream flow accelerates with downstream direction, as the flow expands around the end of the ramp. Measurements of the freestream velocity with the jet turned on were also attempted, but inadequate seeding and low laser power made this task difficult.

Figure 17 provides the velocity profile of the flow with the jet turned on. The recirculation region has vanished, and is replaced with a high velocity wall jet. Between this wall jet and the freestream flow is a lower velocity mixture region near the top of the model. This region probably contains many Kelvin-Helmholtz type structures since it lies in a shear layer region between the main and injected flows. The mass flow rate of the injected flow is slightly more than fifty percent of the main flow since the pressure is only 5 psia. This causes a very profound effect in the base region when the jet is turned on.

Conclusions

Injection after the compression ramp is shown to have a profound effect on the flow. The final expansion fan is displaced upwards, and the base region contains a strong wall jet coupled with the high velocity main flow through a lower velocity mixing region. The recirculation zone behind the ramp, present when the jet is turned off, can be entirely eliminated if the mass flow rate of the jet is high enough.

Interferometry reveals and inviscid calculations reveal that the injected jet is slightly under-expanded at the end of the nozzle, and a series of shocks and expansions are located at the injection outlet. The base region is found to be very turbulent with the jet on, and this should aid in mixing between the injected and main flows. Injection ramps are found to be a viable means to increase mixing between the injected and main streams.

Acknowledgments

With the number of people who provided advice, assistance, and equipment for this project, I fear this section sounds similar to an acceptance speech for the Oscars. Nevertheless, since much of the equipment for this project was borrowed, and since it was difficult, if not impossible, to perform many of the tests without assistance, this project could not have been completed without the help of several individuals. I name many of them now.

I would like to thank my research advisor, Professor Holt, for all of his assistance in this endeavor. I would also like to thank all of the people at Aerometrics; specifically Dr. William Bachalo, Roger Rudoff, and Khalio Ibrhim for the loan and setup of the LDV equipment, as well as instruction on its use and their many hours of assistance during tests. Thanks also to John Woycheese for assisting in the taking of the interferometry photographs, and to Patricia Woycheese for the use of her printer in the printing of this report.

Thanks to John Cavolowsky, who oversaw this project for NASA Ames Research Center, and who provided valuable advice on model setup. Thanks also to Tony Gross who helped secure funds for the completion of this project. Thanks to Professor Chapman for advice on the design of the model and interferometry techniques,. Finally, thanks to my fiancé, Tanya Perefege, for understanding during the long hours of work on this project.

This project was funded under a Consortium with NASA Ames Research Center, grant number NCC2-5190.

References

[1]Heisler, W. H., and Pratt, D. T., *Hypersonic Airbreathing Propulsion*, AIAA Education Series, AIAA, Washington, DC, 1994, pp. 22-26.

[2]Da Silva, L. F. F., Deshaires, B., Champion, M., and Rene-Corail, M., "Some Specific Aspects of Combustion in Supersonic H_2-Air Laminar Mixing Layers," *Combustion Science and Technology*, Vol. 89, 1993, pp. 317-333.

[3]Kwok, F. T., Andrew, P. L., and Ng, W. F., "An Experimental Investigation of a Supersonic Shear Layer with Slot Injection of Helium," AIAA 20th Fluid Dynamics Conference, Buffalo, New York, AIAA Paper 89-1868, 1989.

[4]Belovich, V. M., Samimy, M., and Reeder, M. F., "Dual Stream Axisymmetric Mixing in the Presence of the Axial Vorticity," *Journal of Propulsion and Power*, Vol. 12, NO. 1, Jan.-Feb. 1996, pp. 178-185.

[5]Provinelli, F. P., Provinelli, L. A., and Hersch, M., "Effect of Angle of Attack and injection Pressure on Jet Penetration and Spreading from a Delta Wing in Supersonic Flow," NASA TM-X-1889, Sep. 1969.

[6]Hersch, M., and Provinelli, L. A., "Effect of Interacting Vorticies on Jet Penetration into a Supersonic Stream," NASA TM-X-2134, Nov. 1970.

[7]Swithenbank, J., Eames, I., Chin, S., Ewan, B., Yang, Z., Cao, J., and Zhao, X., "Turbulence Mixing in Supersonic Combustion Systems," AIAA Paper 89-0260, Jan. 1989.

[8]Riggins, D. W., McClinton, C. R., Rogers, R. C., and Bittner, R. D., "Investigation of Scramjet Injection Strategies for High Mach Number Flows," *Journal of Propulsion and Power*, Vol. 11, No. 3, May-June 1995, pp. 409-418.

[9]Kraus, D. K., and Cutler, A. D., "Mixing of Swirling Jets in a Supersonic Duct Flow," *Journal of Propulsion and Power*, Vol. 12, No. 1, Jan.-Feb. 1996, pp. 170-177.

[10]Alzner, E., and Zakkay, V., "Turbulent Boundary-Layer Shock Interaction with and without Injection," *AIAA Journal*, Vol. 9, 1971, pp. 1769-1776.

[11]Peak, D. J., "The Use of Air Injection to Prevent Separation of the Turbulent Boundary Layer in Supersonic Flow," A. R. C. CP No. 890, 1966.

[12]Grin, V. T., and Zakharov, N. N., "Experimental Investigation of the Effect of Tangential Blowing and Wall Cooling on Flow with Seperation," *Fluid Dynamics*, Vol. 6, 1974, pp. 1035-1038.

[13]Childs, M. E., Paynter, G. C., and Redecker, E., "The Prediction of Seperation and Reattachment Flow Characteristics for Two-Dimensional Supersonic and Hypersonic Turbulent Boundary Layers," AGARD Conference Proceedings, No. 4, *Separated Flows*, pts 1 and 2, May 1966.

[14]Juhany, K. A., and Hunt, M. L., "Flow-field Measurements in Supersonic Film Cooling Including the Effect of Shock Wave Interaction," AIAA Paper 92-2950, July, 1992.

[15]Riggins, D. W., and Vitt, p. H., "Vortex Generation and Mixing in Three-dimensional Supersonic Combustors," *Journal of Propulsion and Power*, Vol. 11, No. 3, May-June 1995, pp.419-426.

[16]Waitz, I. A., Marble, F. E., Zukoski, E. E., "A Systematic Experimental and Computational Investigation of a Class of Contoured Wall Fuel Injectors," 30th Aerospace Sciences Meeting and Exhibit, AIAA Paper 92-0625, 1992.

[17]Ju, Y., and Niioka, T., "Ignition Analysis of Unpremixed Reactants with Chain Mechanism in a Supersonic Mixing Layer," *AIAA Journal*, Vol. 31, No. 5, May 1993, pp. 863-868.

[18]Loomis, M. P., "Interferomic Investigations of Supersonic Flow Fields with Shock-Shock Interactions," Ph.D. Dissertation, U. C. Berkeley, 1990.

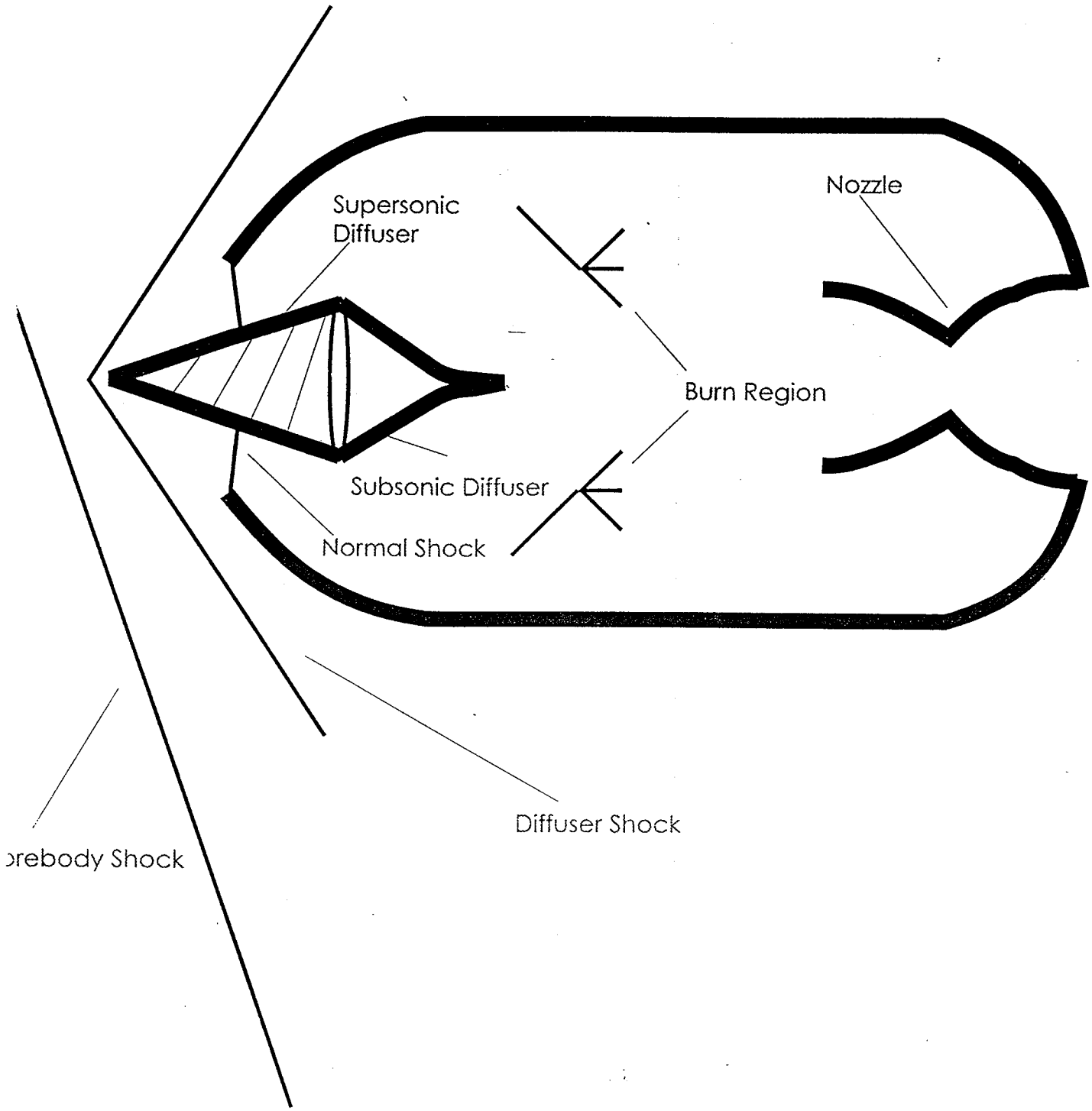

Figure 1: Ramjet Configuration

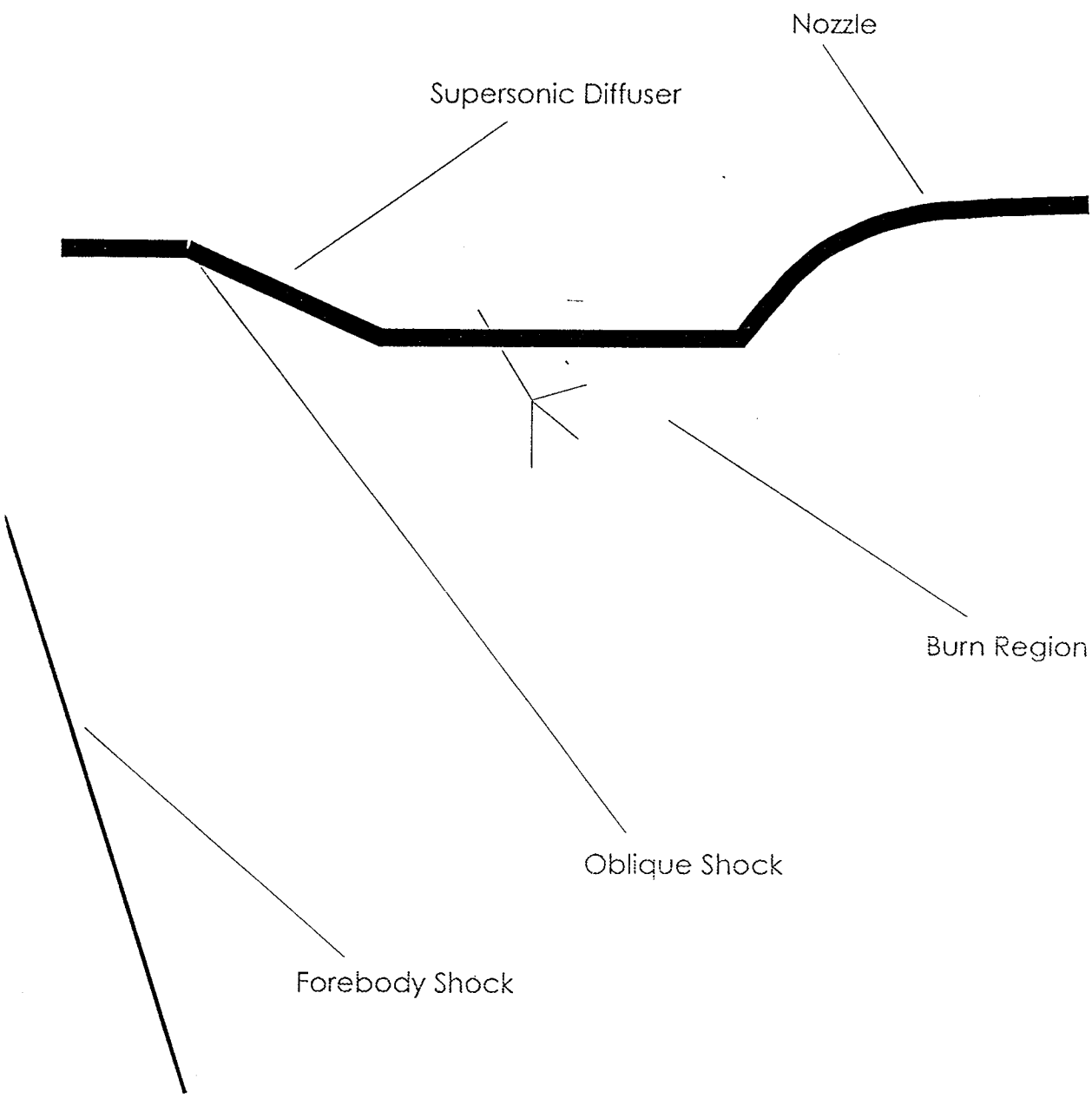

Figure 2: Scramjet Configuration

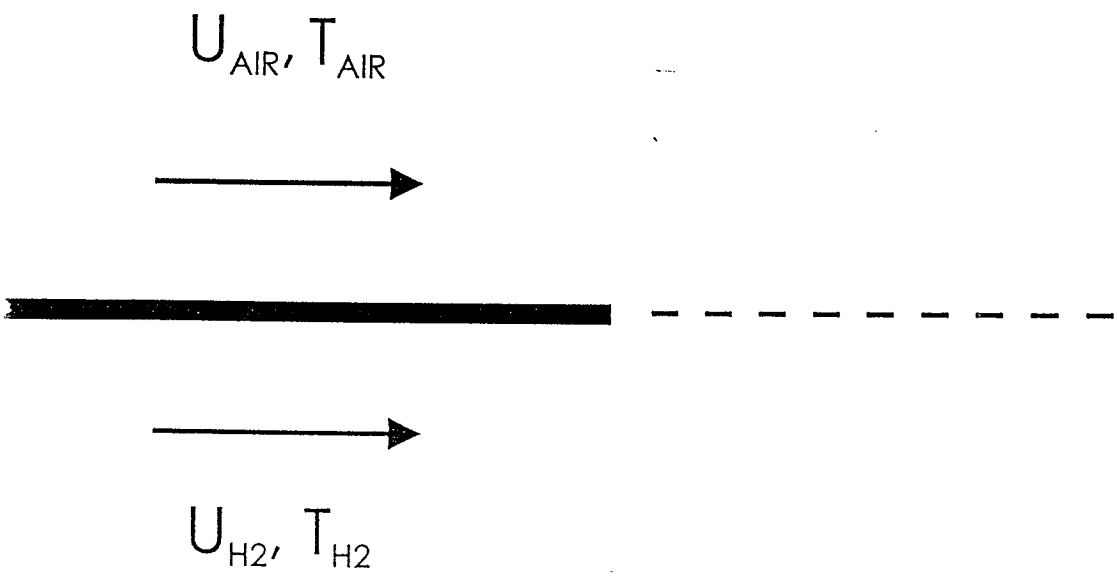

Figure 3: Air/H_2 Mixing Layer

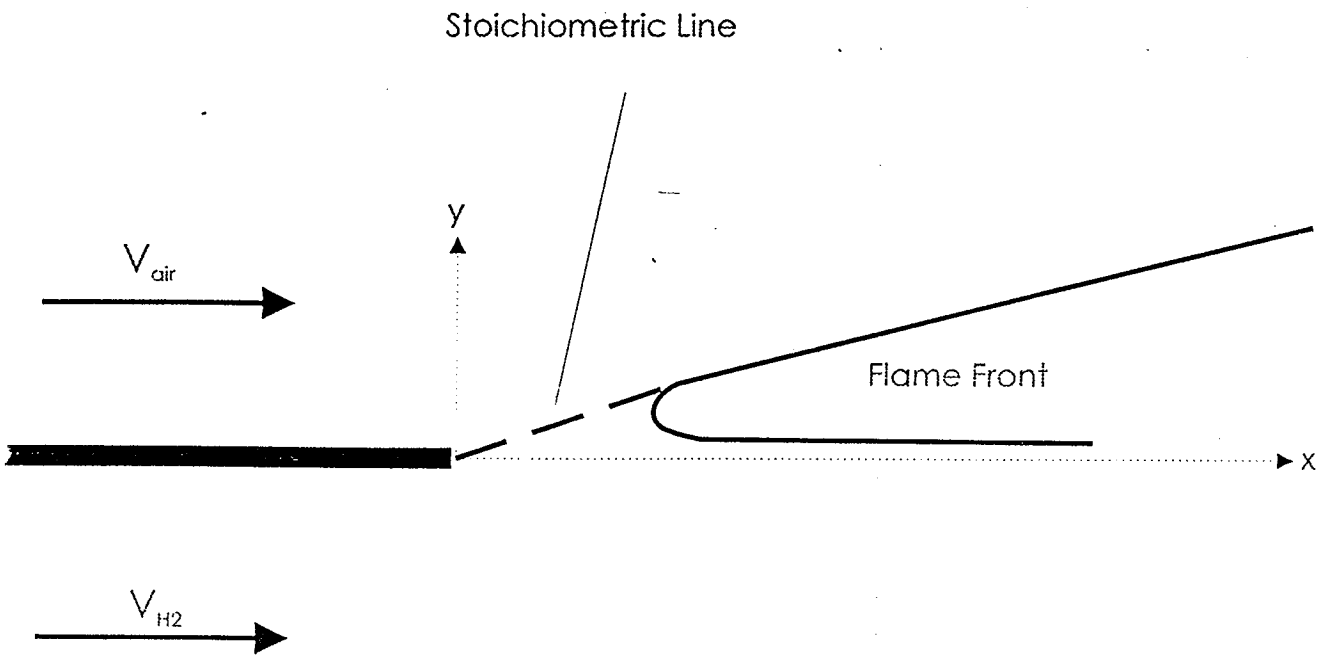

Figure 4: Typical Mixing Layer Schematic[2]

A)

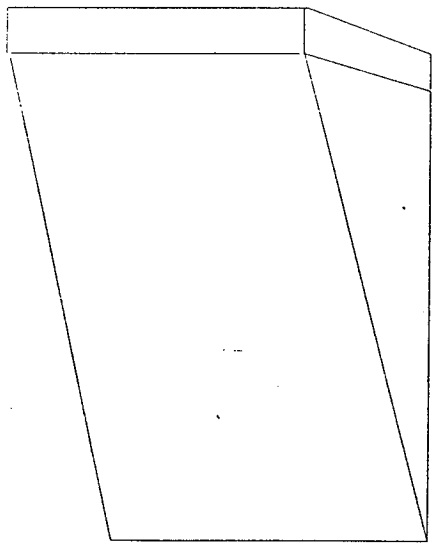

B)

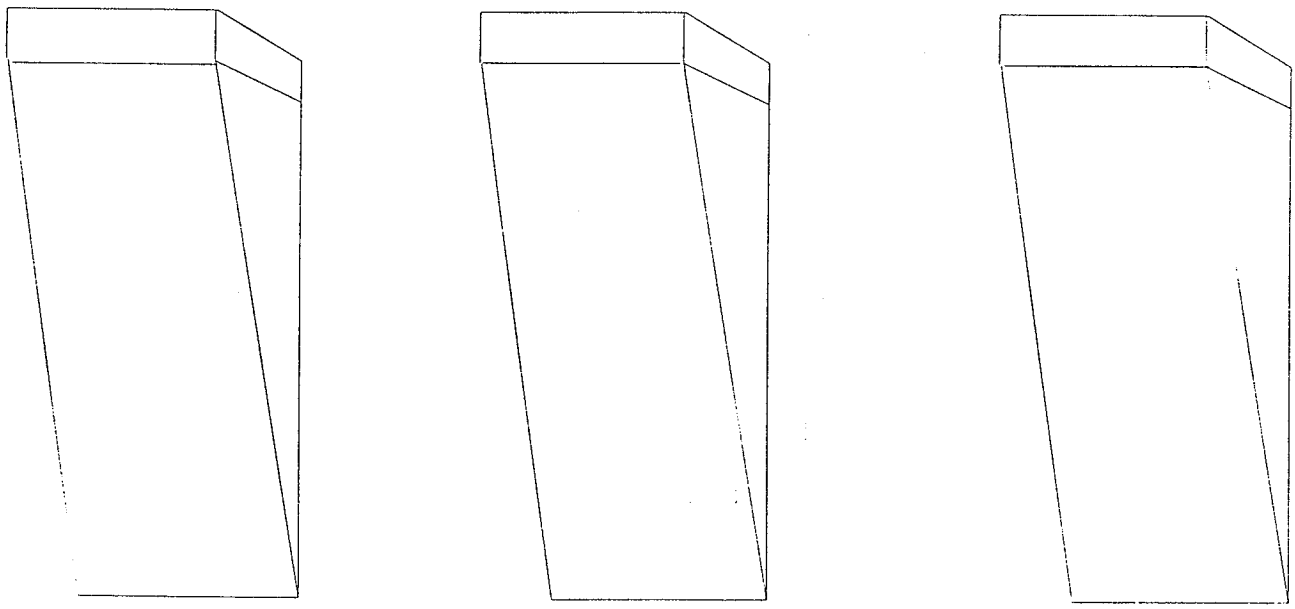

Figure 5: A) Contoured Wall Injector
B) Array of injectors

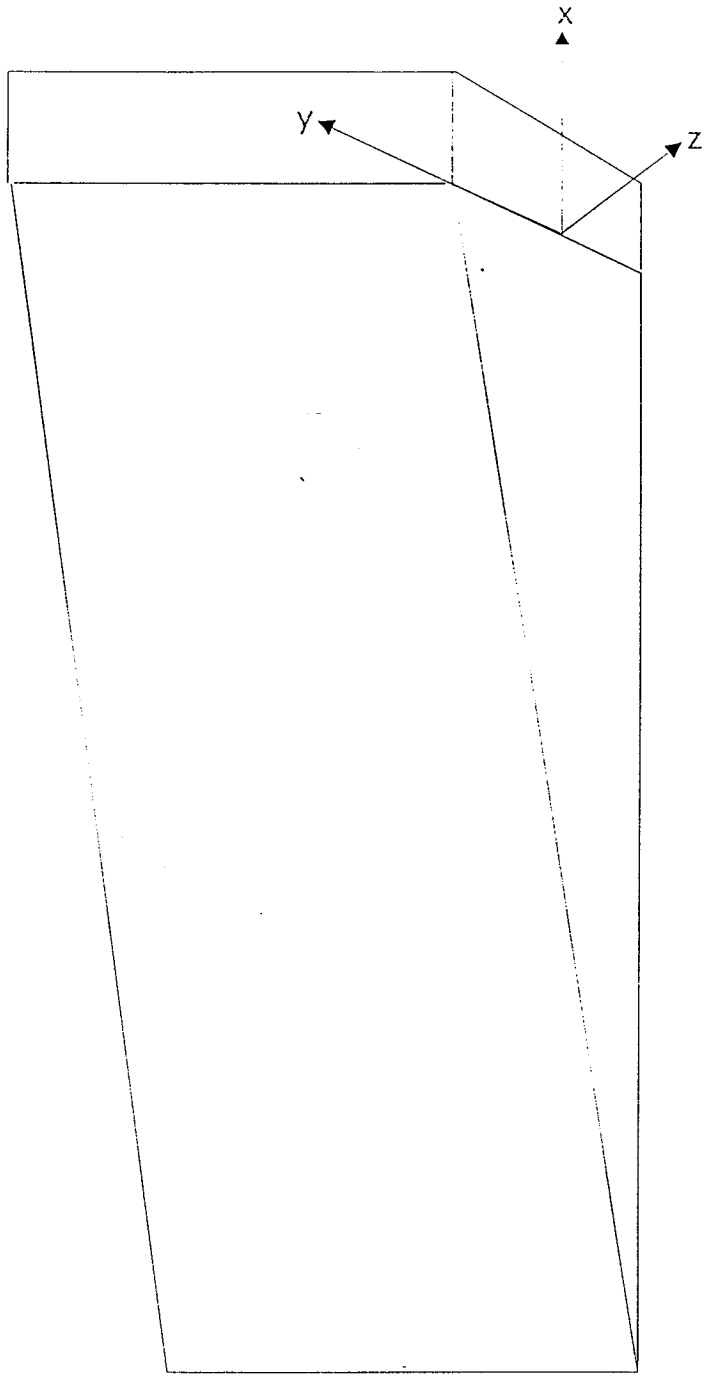

Figure 6: Axes Orientation

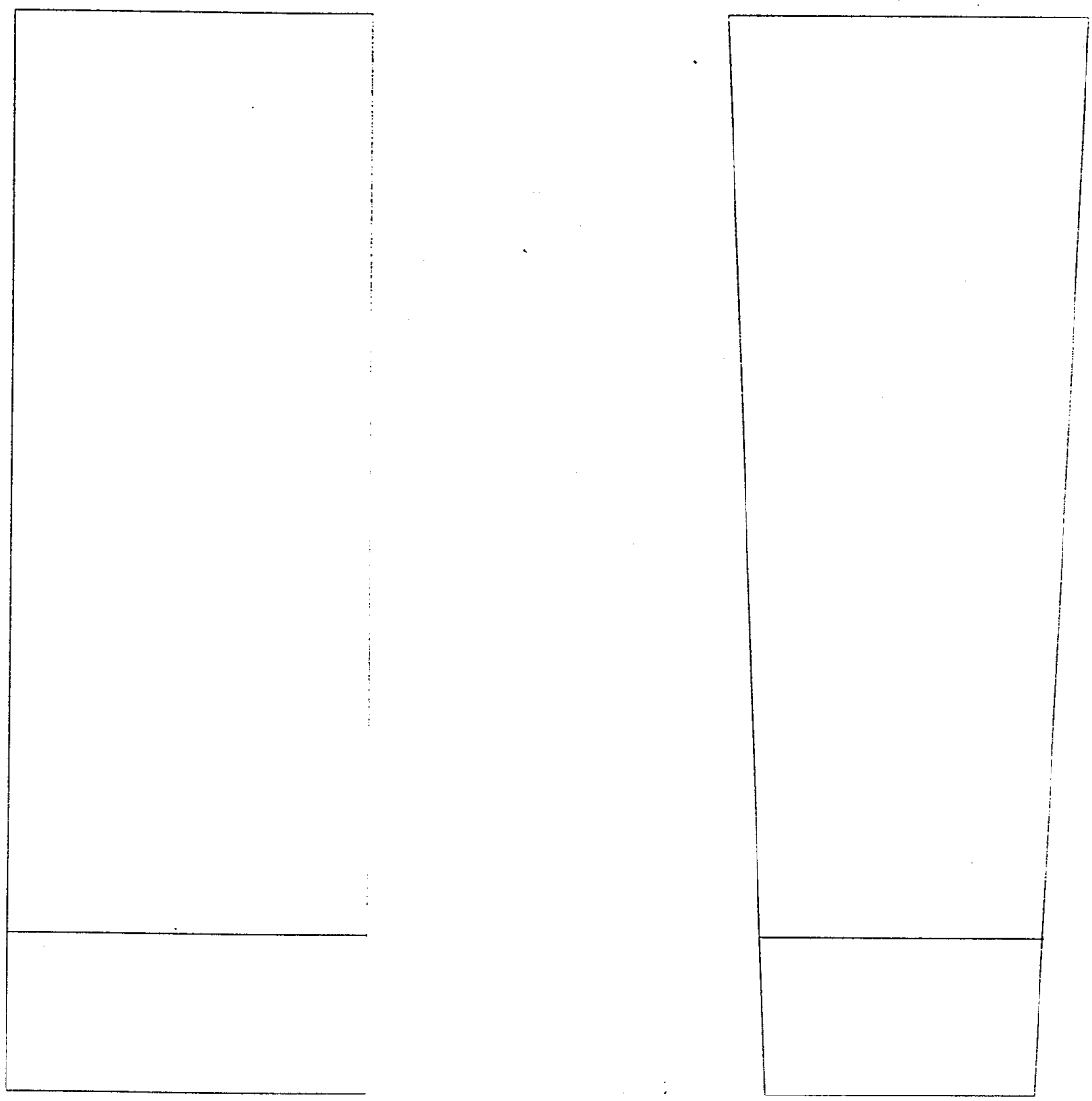

Figure 7: Unswept and Swept Ramps

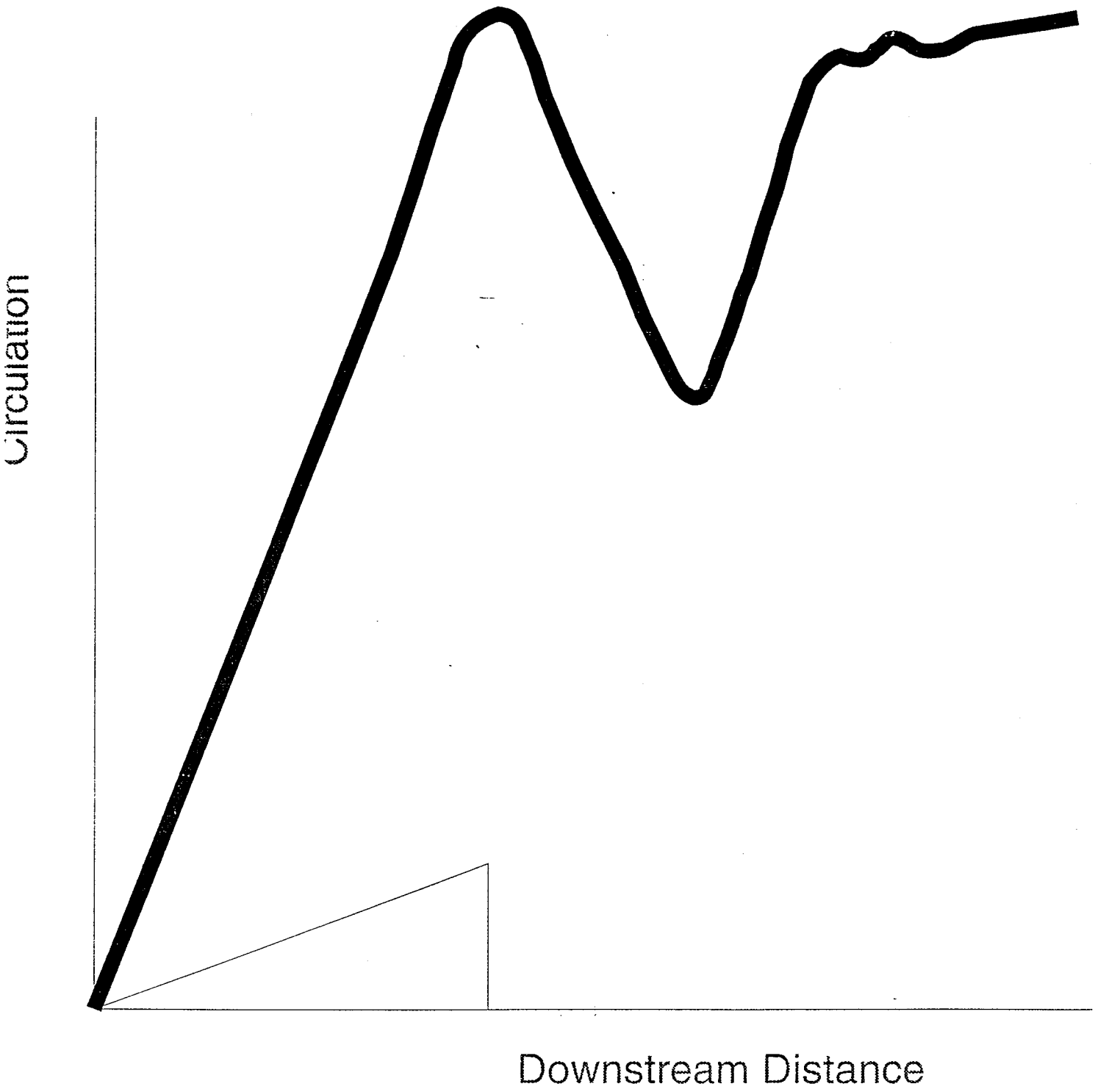

Figure 8: Circulation vs. Distance Downstream[10]

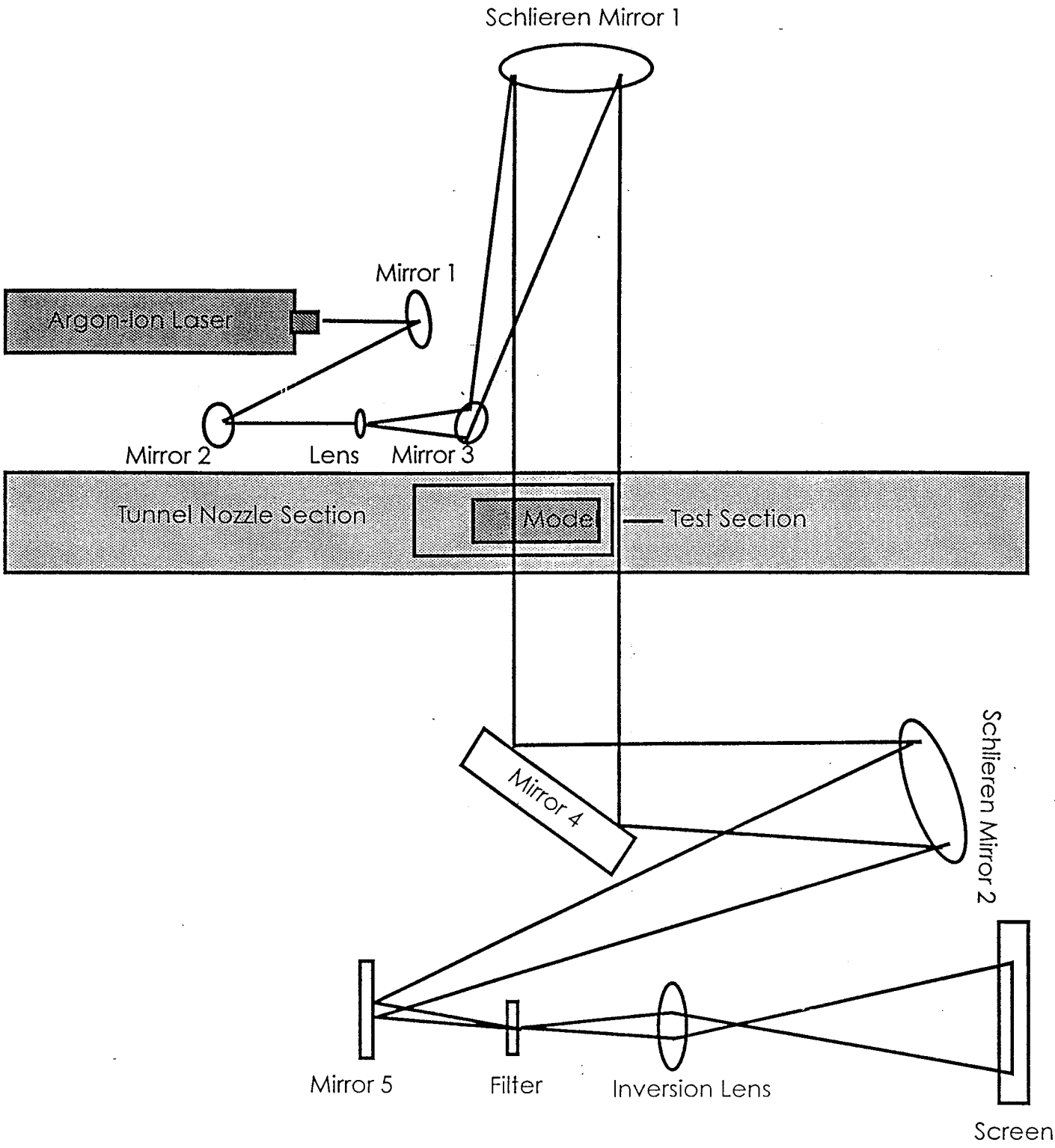

Figure 9: DCGI System Schematic

A)

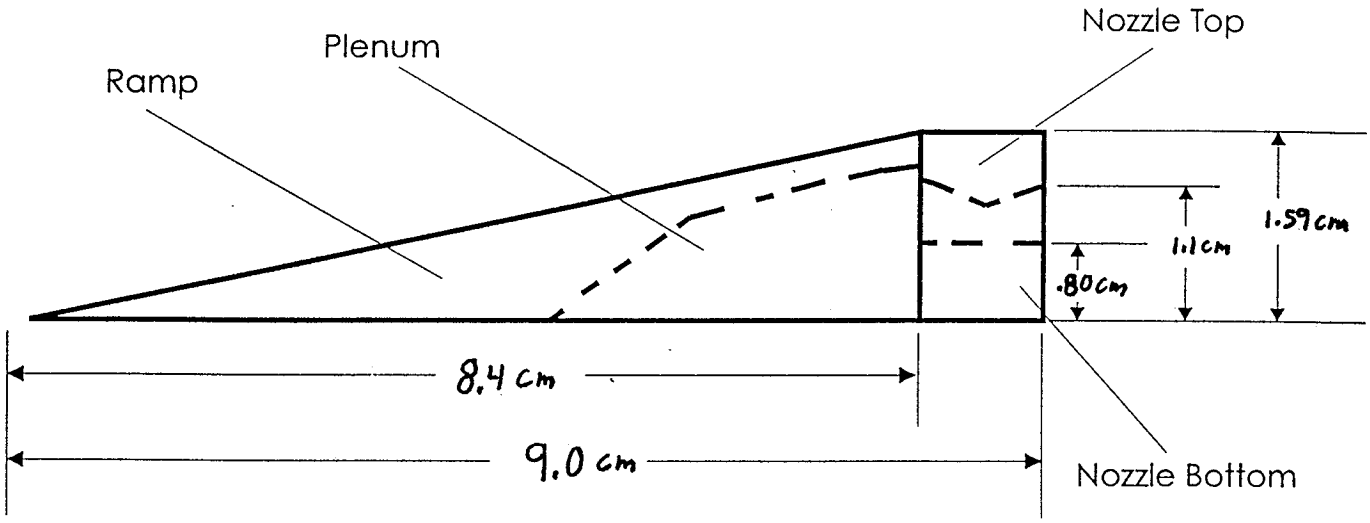

B)

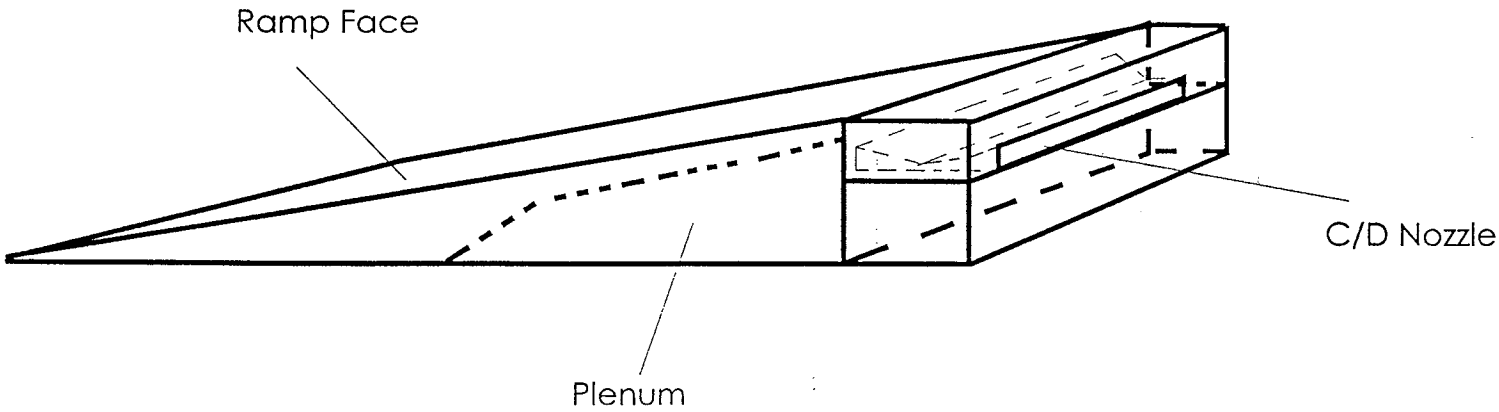

Figure 10: A) Model Side View
B) Model Skew View

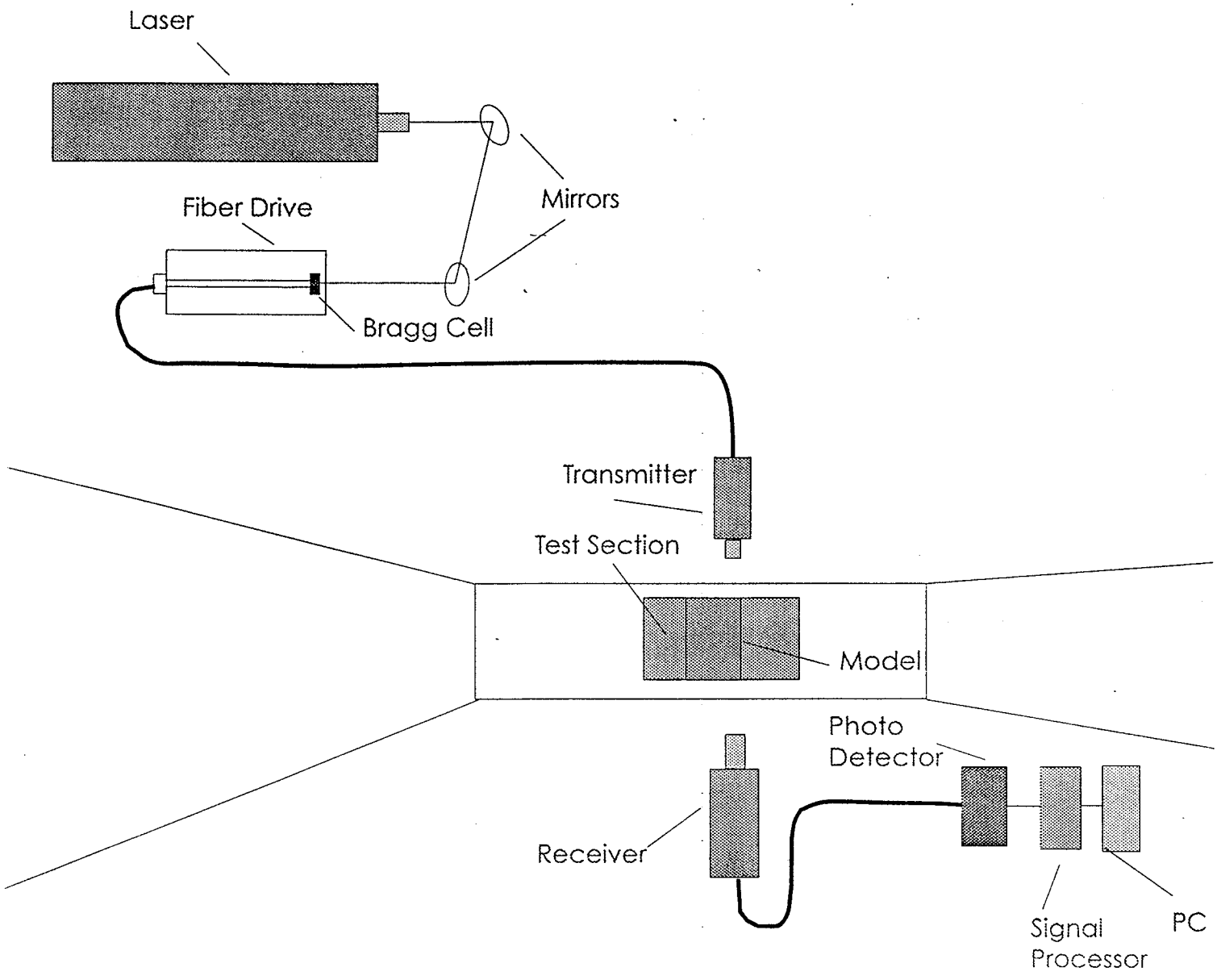

Figure 11: LDV Diagram

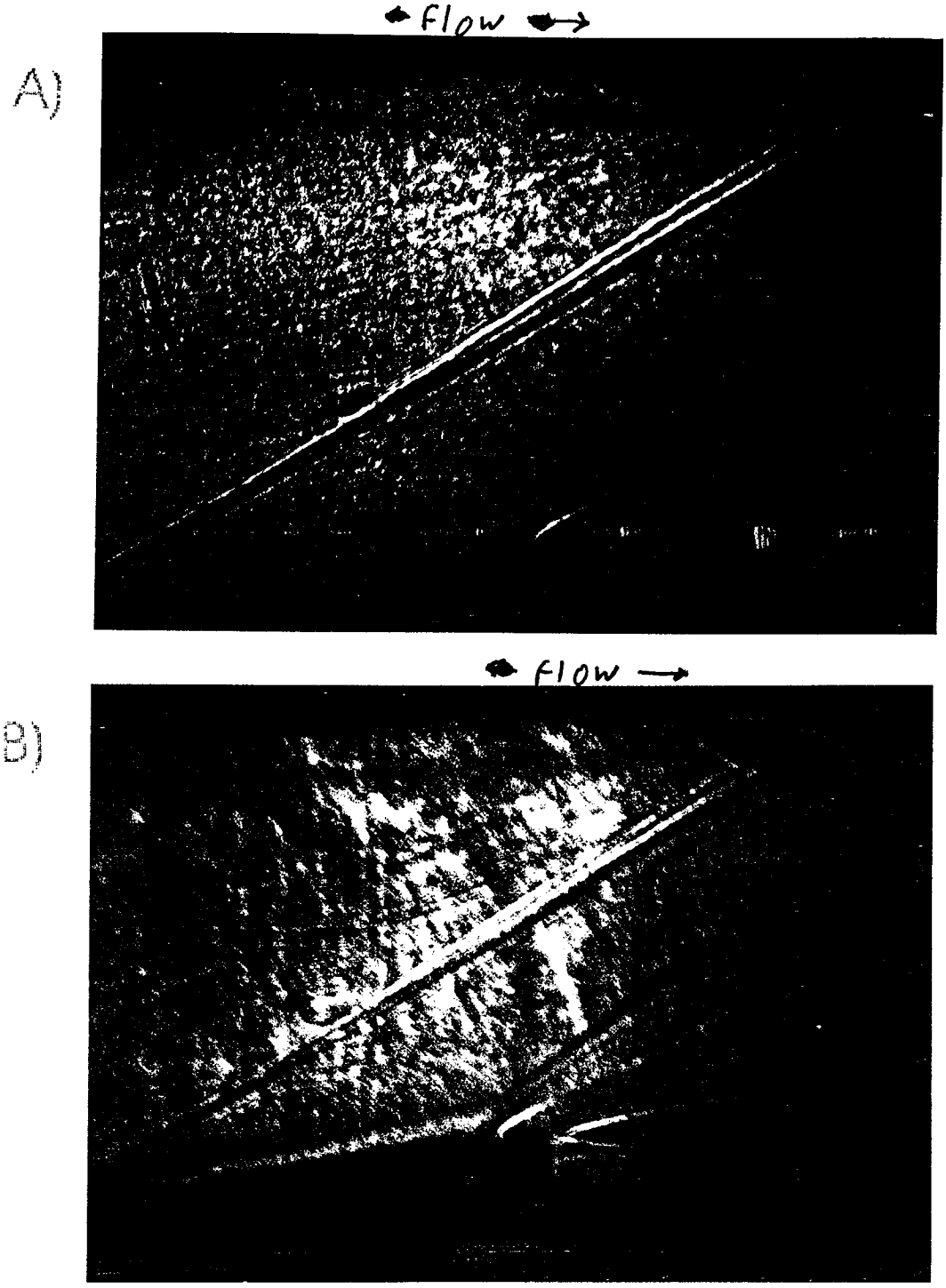

Figure 12: A) Shadowgraph with Jet Off
B) Interferogram with Jet Off

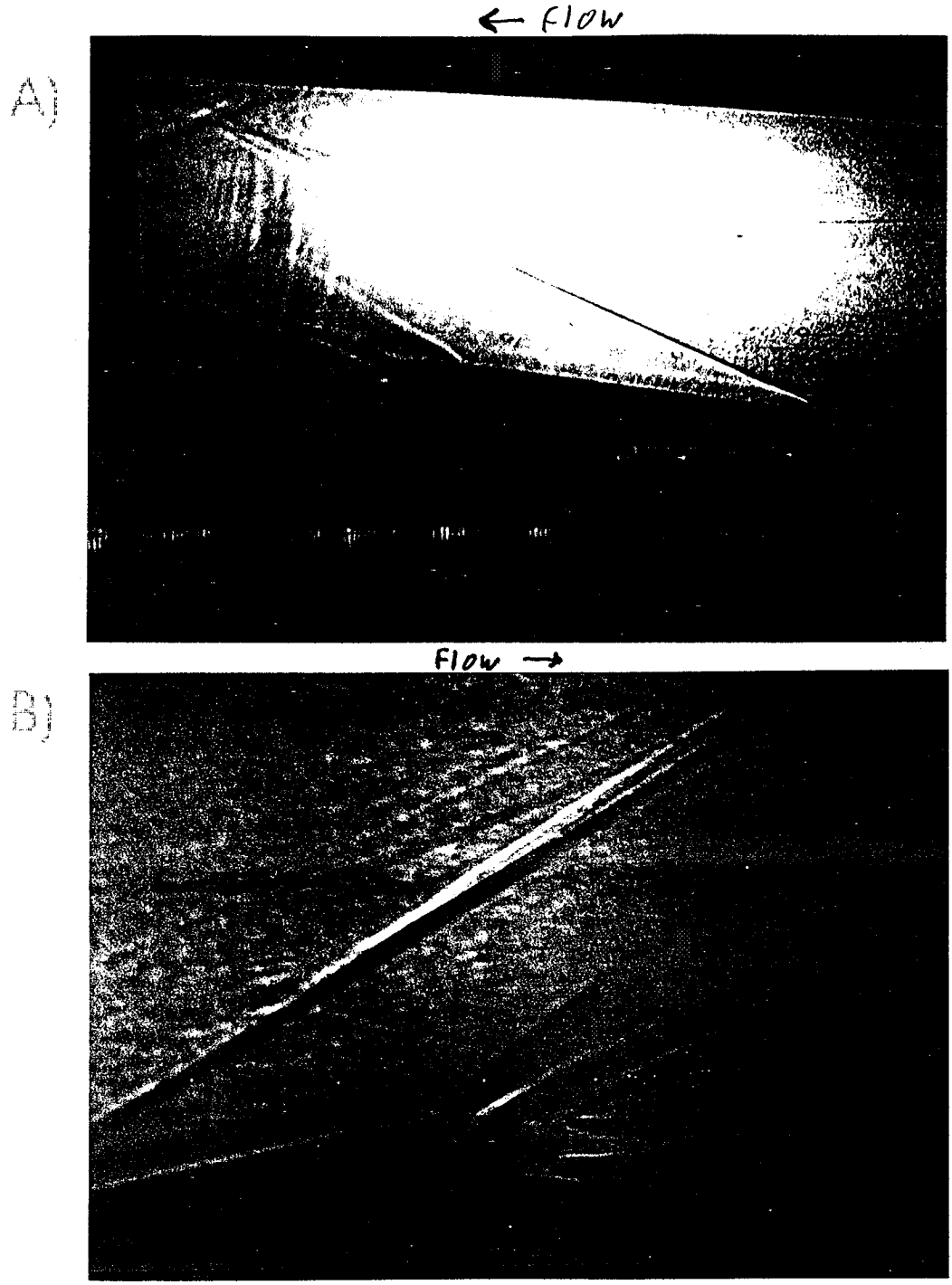

Figure 13: A) Shadowgraph with Jet On

B) Interferogram with Jet On

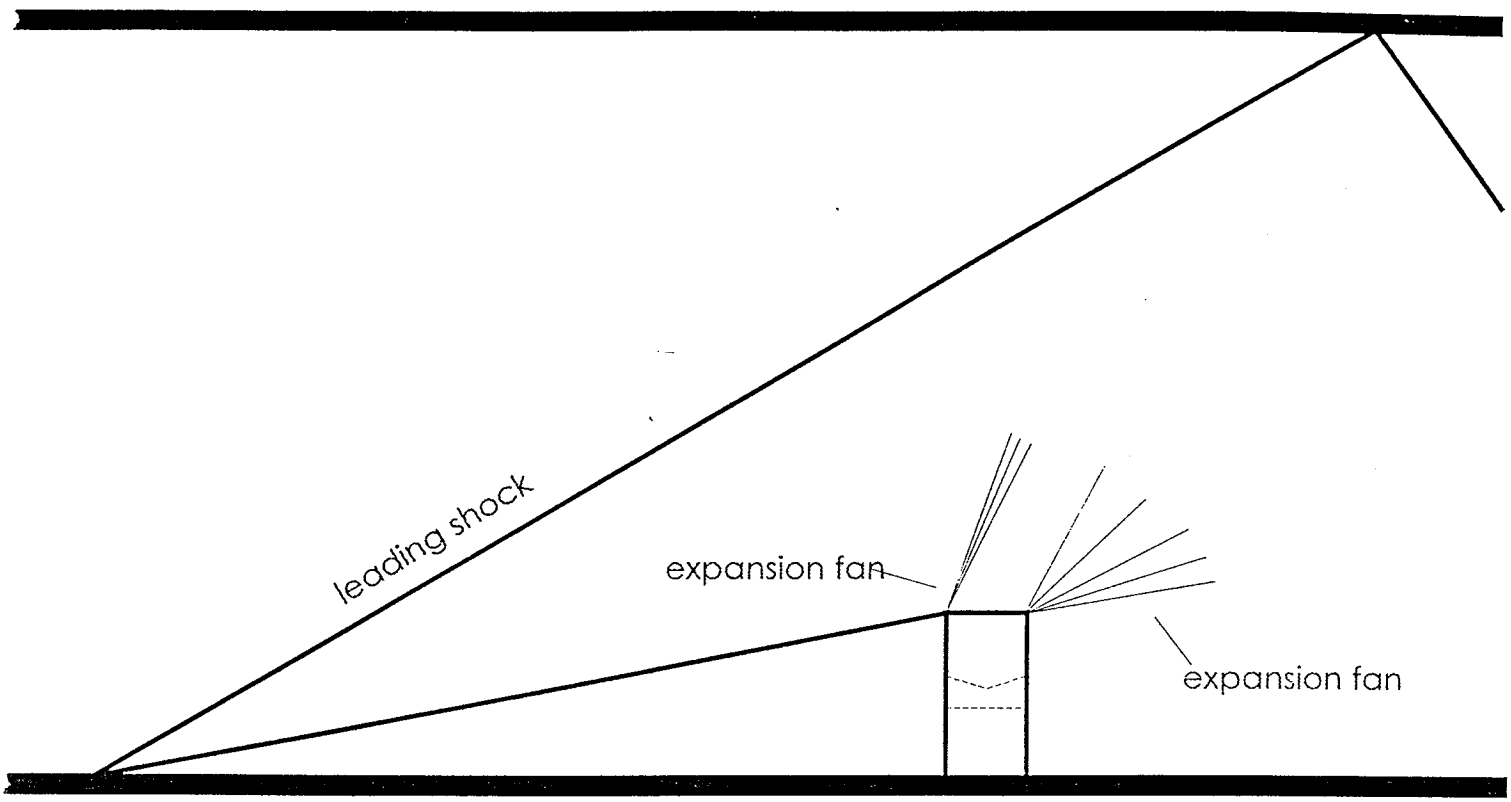

Figure 14: Schematic of Model Without Injection

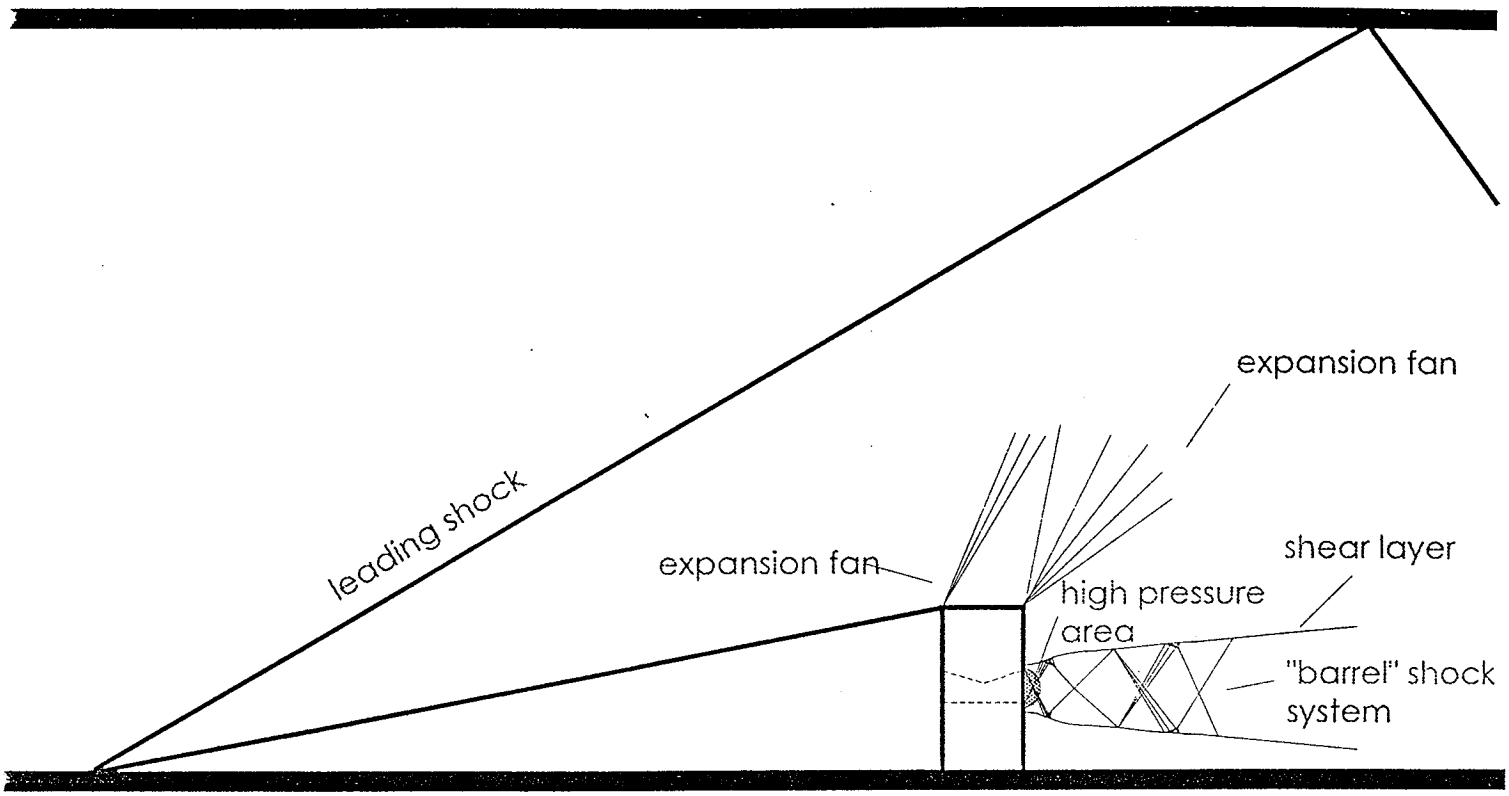

Figure 15: Schematic of Model With Injection

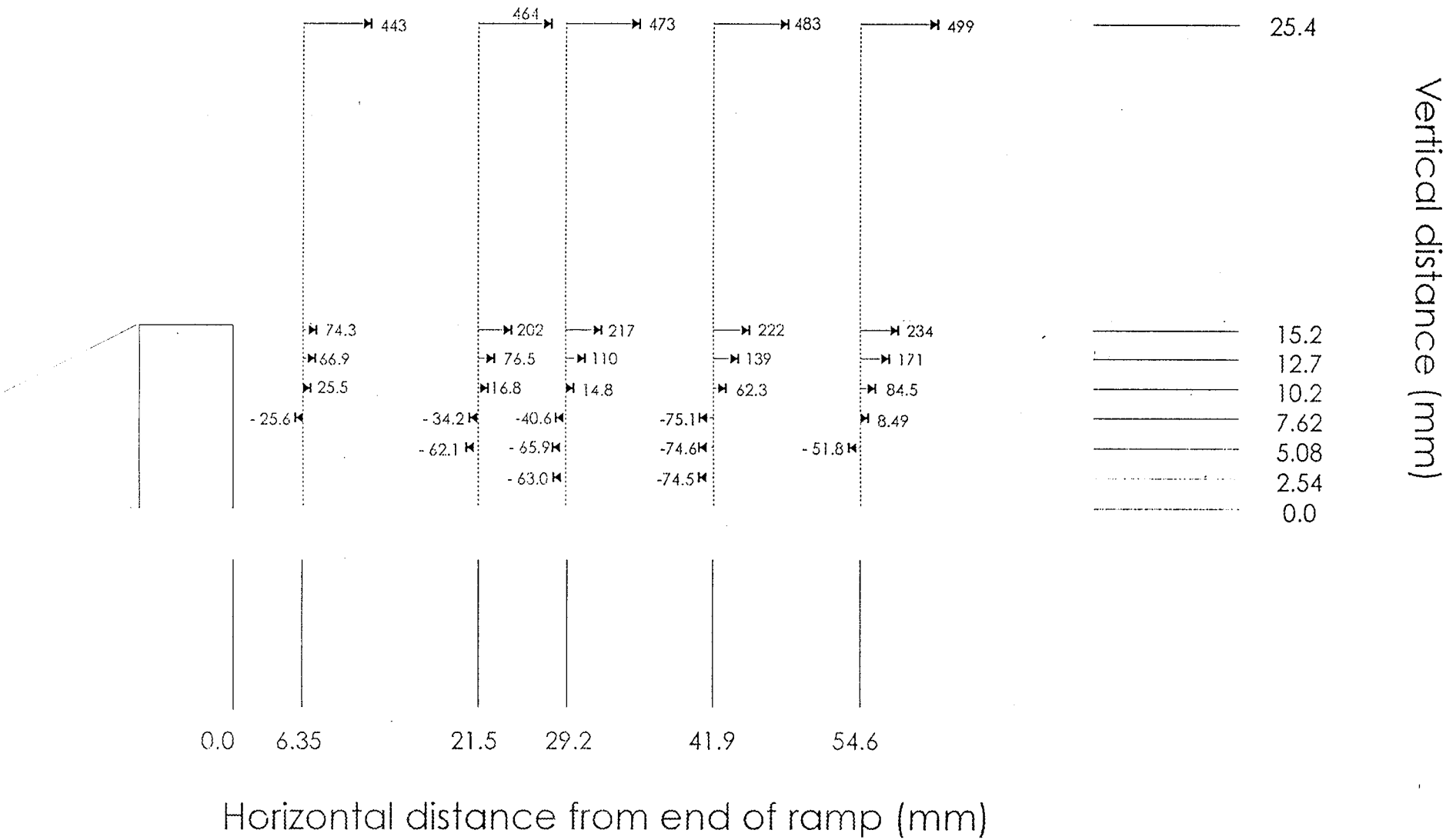

Figure 16: Streamwise Velocity Profile (m/s) with Jet Off

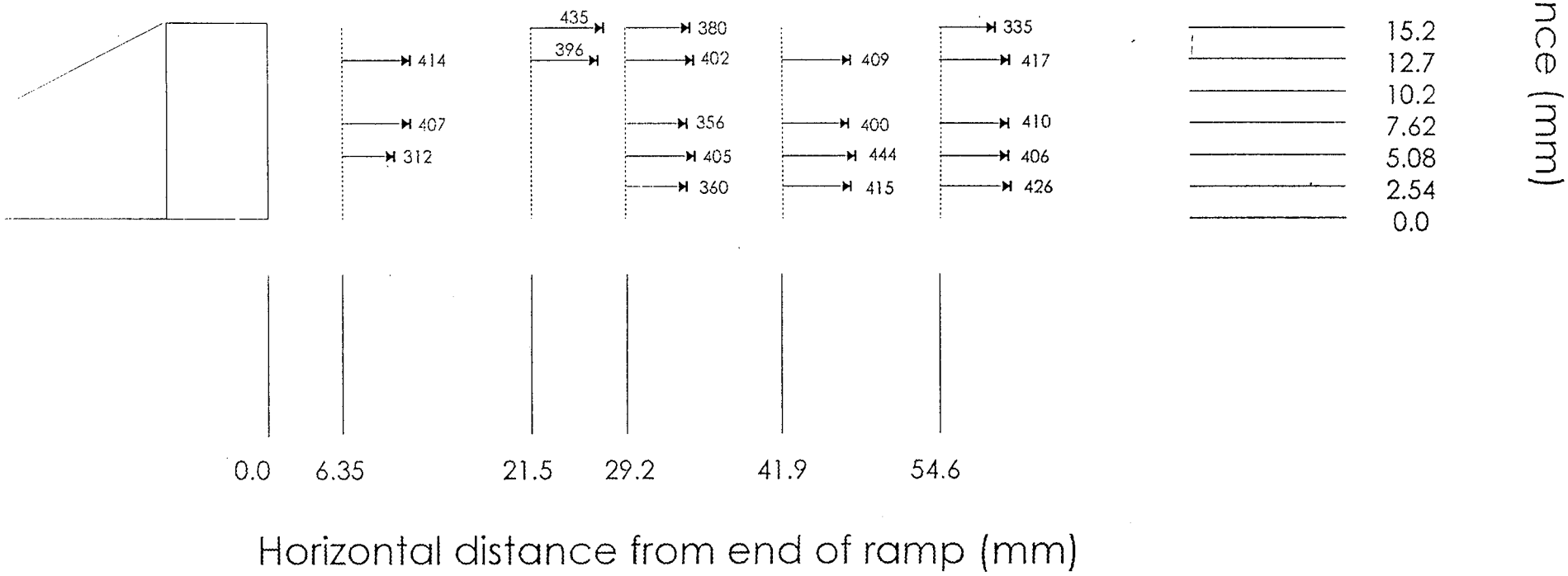

Figure 17: Streamwise Velocity Profile (m/s) with Jet On